THE ANNALS OF “DUNAREA DE JOS” UNIVERSITY OF GALATI
FASCICLE XI – SHIPBUILDING. ISSN 1221-4620, e-ISSN 2668-3156
DOI: https://doi.org/10.35219/AnnUgalShipBuilding/2025.48.17
2025

THE INFLUENCES OF FORCES GENERATED BY WIND AGAINST A FERRY TYPE VESSEL

Andrei Dobrinas
“Dunarea de Jos” University of Galati,
Faculty of Naval Architecture, Galati,
47 Domneasca Street, 800008, Romania,
E-mail: ad399@student.ugal.ro

Radu Bosoanca
“Dunarea de Jos” University of Galati,
Faculty of Naval Architecture, Galati,
47 Domneasca Street, 800008, Romania,
E-mail: radu.bosoanca@ugal.ro

ABSTRACT

The advancement of innovative solutions in shipbuilding demands the ongoing enhancement of research infrastructure. Hydro-aerodynamic challenges related to fluid flow around ship hulls can be addressed using numerical and/or experimental methods. However, numerical results must always be validated through experimental model testing in specialized hydro-aerodynamic laboratories. To support such research, a wind tunnel was developed at the Faculty of Naval Architecture, “Dunărea de Jos” University of Galați, enabling the measurement of aerodynamic forces and moments, as well as the distribution of speed and pressure on the hull under wind action. This paper highlights the main types of problems that can be experimentally investigated in the aerodynamic tunnel and describes the specific experimental equipment used.

1. Introduction

In modern maritime transportation, the demand for fast, fuel-efficient, and environmentally sustainable vessels has led to the widespread adoption of innovative ship designs, including catamaran ferries. A catamaran ferry, often employed for high-speed passenger or mixed cargo transport, operates with unique hydrodynamic and aerodynamic characteristics due to its twin-hull structure and extensive above-water profile. While much attention is often focused on hydrodynamic drag, wind resistance (also known as aerodynamic drag) can constitute a significant portion of the total resistance encountered by a vessel, especially at higher speeds and in exposed sea routes. Therefore, accurately measuring and accounting for wind resistance is essential in optimizing performance, reducing operational costs, and minimizing environmental impact.

Wind resistance becomes particularly important in catamaran designs because of the relatively large frontal and side surface areas presented above the waterline, which can interact with ambient wind conditions. These interactions not only influence fuel consumption but also affect vessel stability, manoeuvrability, and passenger comfort. Moreover, for ferries operating on fixed schedules and under varying weather conditions, understanding the impact of wind resistance is vital for ensuring reliable journey times and safe operations. Even modest improvements in aerodynamic efficiency can translate into substantial savings over time, both in terms of fuel usage and emissions reduction, aligning with global efforts to decarbonize the maritime industry.

Furthermore, wind resistance data supports the development and refinement of predictive models for ship performance, enabling more accurate route planning, load distribution, and propulsion system optimization. It also plays a critical role in ship design processes, where computational fluid dynamics (CFD) simulations and wind tunnel testing can be used to evaluate and enhance the aerodynamic profile of the ferry. As international maritime regulations continue to tighten around emissions and energy efficiency—such as the IMO's Energy Efficiency Existing Ship Index (EEXI) and Carbon Intensity Indicator (CII)—the need for precise measurements of all forms of resistance, including wind-induced drag, becomes increasingly pressing.

In conclusion, measuring wind resistance is not a peripheral concern but a central element in the operational and design optimization of a vessel. Through accurate assessment and strategic mitigation of wind drag, ship operators can achieve significant gains in efficiency, safety, and environmental compliance [1].

2. Aspects regarding the generation and selection of model ship dimensions

To choose the dimensions of the model ship, different ships of the same category were studied.

Table 1 Similar ships

Ship Name	L	B	T	Δ	Cars	People	Dwt	Speed	Power
	[m]	[m]	[m]	[mt]	No.	No.	[mt]	[kn]	[kW]
Queen of Capilano	95.7	21.2	5.8	2500	100	457	602	12	7305
Aqua Jewel	96.0	16.6	7.7		160	661	461	18	6358
Coho	93.9	21.9	6.2		110	1000	2057	15	5100
Veteran	81.1	17.2	6.7		70	200	905	14	5100
Alfred	84.5	22.0	5.3		98	430	550	16	3348
Pentalina	70.6	20.2	5.0	930	80	350	360	17.1	3580

After analysing the characteristics of different ships of a similar type to the one chosen for the study, the dimensions selected were those recommended by the Maxsurf program, because they respect the constructive pattern of the ship type and are determined based on a well-established database [3].

For the ship studied in the paper, the following main dimensions were established:

Table 2 Main characteristics of the vessel

Ship type	Ferry
Length overall (L_{OA})	90 [m]
Length at waterline (L_{WL})	85.655[m]
Breadth (B)	26 [m]
Construction height (D)	15 [m]
Displacement	734.5 [t]
Draught (T)	2.6 [m]
Speed	20 [Nd]

2.1 Generating the 3D model using the Maxsurf program

To generate a 3D model the Maxsurf database was used. Thus, using the 'Design QuickStart' menu by selecting the desired ship type, it automatically designed a ship that met the required criteria.

As a result, the model was automatically generated using the Maxsurf program, thus meeting the constructive requirements for ferry-type passenger transport vessels.

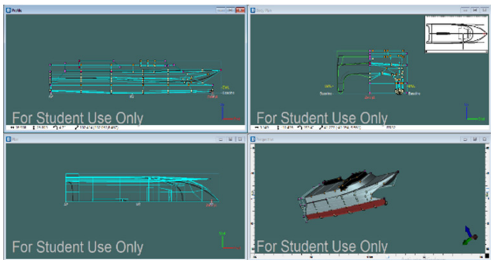

Fig.1. Ship lines plan

3. Printing and preparing the model for testing

3.1 Current 3D printing methods

3D printing is also known as additive or generative manufacturing. The idea behind this manufacturing process is to convert a numerical model into a three-dimensional model or experimental model. It is also a primary casting manufacturing process, which means that a solid body is produced from a shapeless one by successively adding layers of material. The digital data is generated through CAD modelling, data from 3D scanners or 3D modelling, although the 3D printer cannot read this data directly. This in turn requires special software that translates the geometric shape into the printer's machine language using "G-code".[2]

3.2 Processing the 3D model for printing

To print the model to the desired dimensions, it was modified to a scale of 1:130. This scale was chosen to exploit as much as possible the maximum width allowed by the naval wind tunnel (T.A.N.) of the laboratory used, 700 mm. Following the modification, the model reached a maximum length of 692 mm, to be able to rotate the model with 90˚ for transverse wind.

The next step was to remove the submerged part of the ship because the experimental work is carried out exclusively on the emerged ship area. After which the ship had to be divided longitudinally into 3 equal sections to fit on the bed of the used printer, the maximum allowed size being 350x350 mm.

To edit the 3D model, the Rhinocerous 3D application was used.

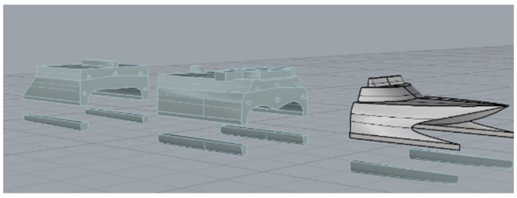

Fig.2. 3D Sections

To facilitate bonding and ensure continuity between sections, a number of cylindrical bodies with dimensions L=10 mm, R=5 mm and corresponding cutouts with the same dimensions were designed.

Points from the half-breadths table were interpolated in Rhinoceros to generate the transverse curves, keel, and deck line. Surfaces were smoothed using the "Smooth" command, and the geometry was checked with "Check," "Zebra," and "Show Edges" for continuity and topological correctness.

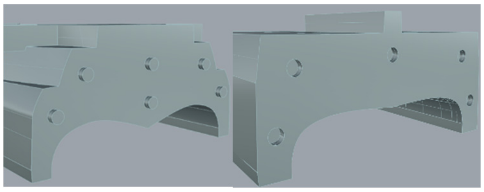

Fig.3. Cylindrical overhang / cut-out

3.3 Printing sections

After processing the model according to the above requirements, the sections were imported one by one into the 3D printer program, Creality Print, to make the final changes before the printing process.

The first step was to select the printer model used for printing and its bed.

The second step was to import the bow section into Creality Print. It was oriented with the bow peak in the positive Z-axis direction to save material needed for supports in non-planar areas and also for an easier construction approach.

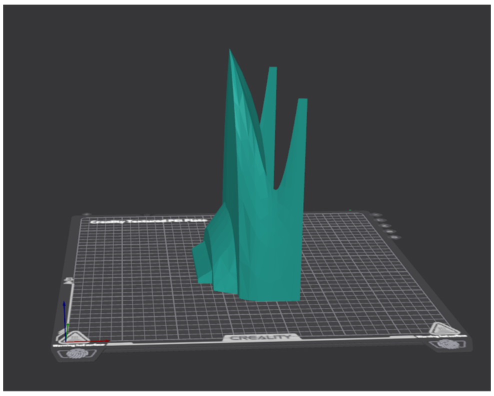

Fig.4. Fore Section

The third step was to select the type of filament used, then the wall thickness represented by the number of passes of the filament and the fill level value expressed in percentage. For the wall thickness, the value of 5 passes (Wall loops) was chosen, and for the fill level, 15% was chosen to add increased rigidity to the model.

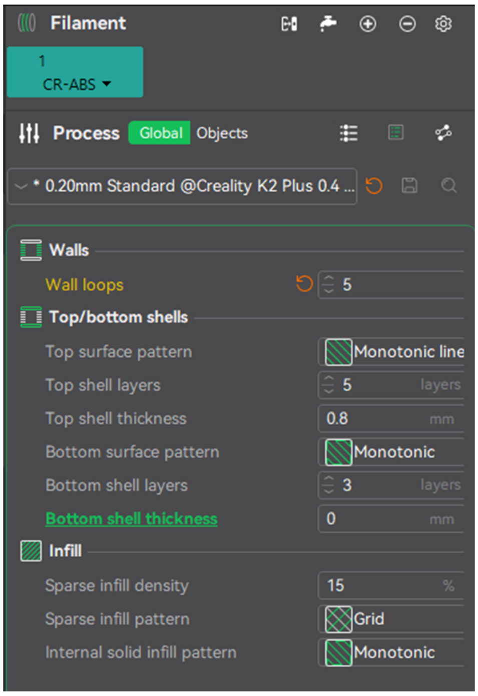

Fig.5. Parameter menu selection

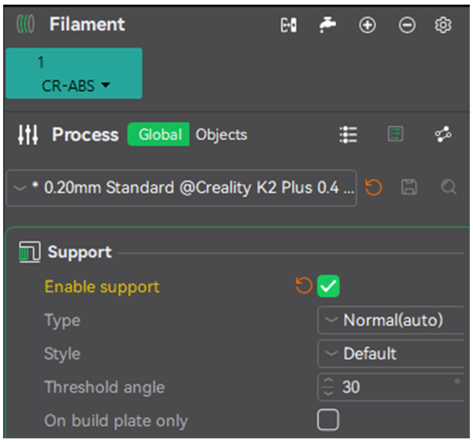

Fig.6. Menu for generating the supports

The automatic support generation feature has also been enabled to help with printing in elevated areas without support.

The last step was to select the preview option which presented the final model and all its features such as the printing time and the total weight of the section. After a final check of the features, the Send print button was pressed and the printing of the respective section was started.

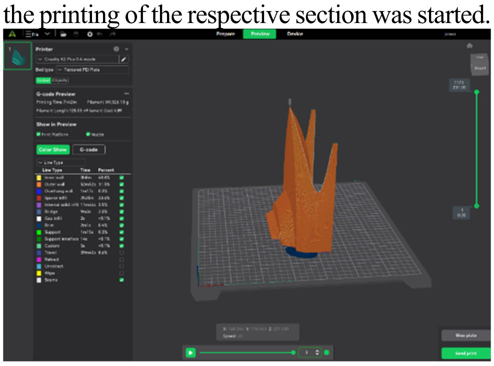

Fig.7. Preview of fore section

After printing the part in the bow area, the process was repeated for the next 2 units.

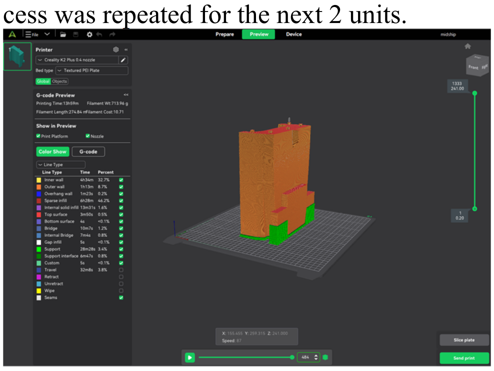

Fig.8. Preview of middle section

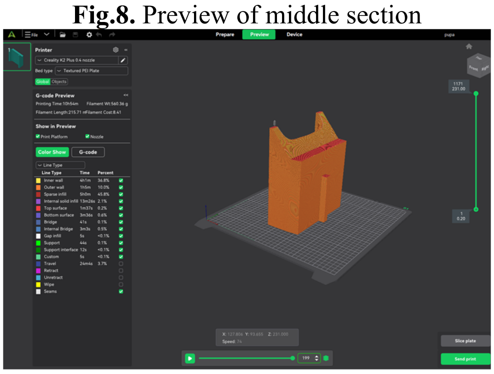

Fig.9. Preview of aft section

4. Preparing the printed model for testing

After printing all the sections, they were glued together with a two-component resin using the specially designed cutouts.

Fig.10. Model ship assembly

For a better finish and to prevent the connection lines from being visible, we used a very fine polyester putty, thus ensuring the continuity of the ship's shape.

5. Aerodynamic testing process

5.1 Selecting norms for testing

In order to achieve the most accurate testing of the influences of environmental factors, it was decided to carry out the tests in accordance with the specific navigation area of the model ship.

Following the study of similar ferry vessels, it was decided to select a known pre-established route as the operating area. Since this had been studied appropriately from a meteorological point of view and in this way, high accuracy data was taken.

Thus, the Port Angeles, Washington – Victoria, British Columbia route was chosen. This connects the U.S.A. and Canada with a distance of 22.6 nautical miles.

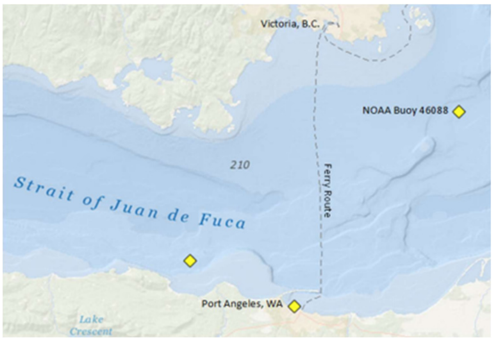

Fig.11. Navigation line Port Angeles, WA – Victoria, B.C. [3]

For a more realistic analysis, the weather conditions in the area such as average and maximum wind speed were analysed. Thus, it was decided to use the maximum wind speed recorded in the last 5 years, 37 mph – 16.54 m/s, for this experiment [8].

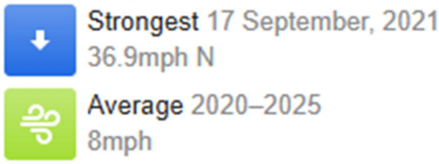

Fig.12. Average and maximum wind speed [8]

5.2 Model testing

For testing, a 30° step was used starting from an incidence angle of 0°, so the incidence angles are as follows: 0°, 330°, 300°, 270°, 180°, 150°, 120°, 90°.

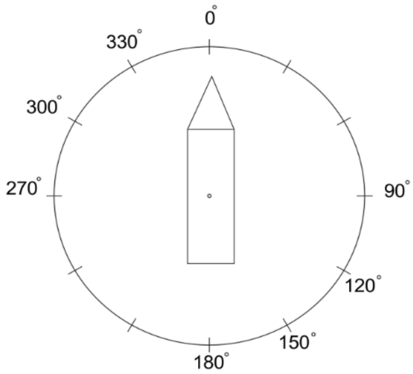

Fig.13. Graphical representation of the incidence angles

Table 3 Measured data

Dyna-mometer	D6	D5	D4	D3	D2	D1
Incidence angle	x	y1	y2	z1	z2	z3
0˚	0.688194	-0.3737	0.178668	17.10444	6.662684	10.29442
90˚	0.387062	-2.95128	-2.20191	23.1407	9.219507	8.707624
120˚	0.548832	-2.91071	-1.30148	20.26795	6.702543	8.593885
150˚	-2.15796	-2.24787	-2.21507	13.18569	8.927133	7.836251
180˚	-2.51214	2.311067	-0.09315	21.07584	7.541433	13.54994
270˚	0.645499	-2.39379	-2.25341	22.25331	8.079659	9.08343
300˚	1.329995	-3.62156	-1.30012	20.57031	6.318256	8.465786
330˚	0.652847	-2.2807	-0.7882	20.1621	5.497399	9.244698

To fix the model in T.A.N. it was screwed to the base of the balance in such a way as to avoid its support on the tunnel bed.

After fixing the model in T.A.N. the testing process was started by starting the engine and respecting the previously established operating range. Following the data recording of the six-component balance and the Pitot tube.

Using the special recording programs of the balance and the tunnel, we took the average pressure value from the Pitot tube by recording 1000 values per second in an interval of 5 seconds and the average of the signals recorded by the balance in the same interval.

After obtaining all the data, they were centralized in a table to be more easily entered into the data processing application.

Table 4 Measured data (continue)

Dynamometer			
Incidence angle	Pa	Rpm	v (m/s)
0˚	149.2839	750	15.74084
90˚	141.7229	750	15.33704
120˚	137.3418	750	15.09812
150˚	151.242	750	15.84374
180˚	163.7085	750	16.48379
270˚	137.7139	750	15.11856
300˚	128.2	750	14.58698
330˚	136.5602	750	15.0551

5.3 Tests results

In order to process the data recorded by the equipment used, it was necessary to obtain all the input data used by the special data processing application [4].

The required input data are: Arm (Distance from the centre of gravity of the balance to the model grip), angle of incidence, wind speed, frontal surface of the model, model length, air density at the relevant temperature on the day of testing (20˚C), calibration constants, inverse of the interdependence matrix from the calibration and the data measured by the six-component balance [5], [6], [7], [9], [10].

The arm was measured using a tape measure and resulted in 0.28 m.

For the frontal surface, the Rhinocerous 3D program was used, with the help of which the value 0.088527 m2 automatically resulted.

After determining all the input data, the data processing process was started to obtain the aerodynamic forces and moments and their coefficients.

Thus, the data related to the 0˚ angle of incidence were entered:

Table 5 Calculation data sheet

Arm	Beta	V_w	Sf	Al	Ro
-0.28	0	15.74084019	0.088527	0.692	1.26
2.986	6.754	9.441	12.417	0.489	5.545
1.11557	-0.02519	-0.0519	0.02296	-0.08093	-0.16679
0.01681	0.98751	0.01167	0.02004	-0.0624	0.01389
0.03973	0.09769	0.99949	-0.01466	0.01211	0.00625
0.01141	-0.66177	0.01097	0.98664	0.02813	-0.0144
-1.26954	0.02732	0.07191	-0.0215	1.09205	0.2304
-0.15893	0.00681	0.02586	-0.00123	0.00302	1.02365
10.294424	6.662684	17.104439	-0.373697	0.178668	0.688194
D1	D2	D3	D4	D5	D6

Following data processing, a comparative analysis was performed to highlight the influences of forces and moments on the ship's hull depending on the angle of incidence exploited during testing [5].

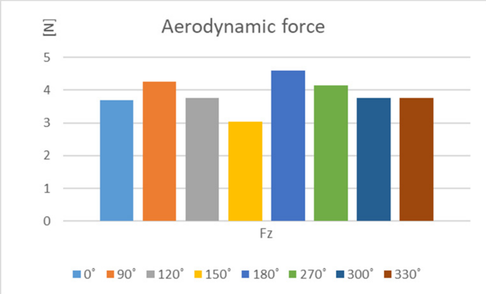

Fig.14. Graphical representation for the vertical aerodynamic force

In the figure above we can see that the most significant influences recorded were those on the z-axis, reaching a value greater than 4.5 N. At the same time, we can see that the results are not very different from one angle of incidence to another.

From figure 15 it can be seen that for the moment My the highest values were recorded, exceeding 14 Nm. It is also worth noting that the maximum value was measured at the 180˚ angle of incidence, and in contrast, negative values were measured at the 90˚ and 150˚ angles.

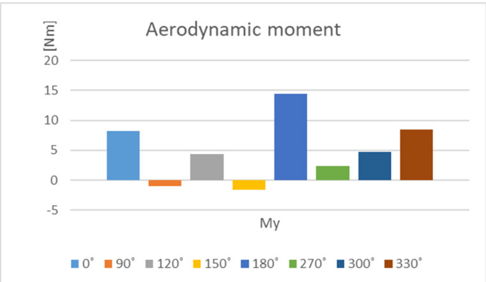

Fig.15. Graphical representation for the vertical aerodynamic moment

6. Conclusions

To determine the aerodynamic resistance, the experimental modelling of the studied ship was carried out, using as inspiration the specifications of several ships in the same category. Thus, a 3D model was designed using specialized software. Subsequently, using the similarity criteria, an experimental model was printed using a 3D printer.

The testing laboratory was prepared in advance by correctly calibrating all equipment, such as the six-component balance and the naval wind tunnel.

At the same time, for this study, a navigation area corresponding to the tested ship was carefully selected in order to generate a simulation close to nature.

Following the modification and preparation of the resulting model, it was used in T.A.N. to measure the total aerodynamic resistance at different angles of incidence.

In conclusion, after respecting all the calibration methodologies and using the equipment used, all the results recorded by them were obtained, centralized and compared.

As a result, the aerodynamic torsion could be calculated at each angle of incidence studied.

7. References

[1]Lisnyk, D. J. (2024). Student Ship Design Competition. Winning Design.
[2](***). Preluat de pe https://www.awi.ro
[3](***). Preluat de pe https://www.3dinbox.ro
[4]Obreja, D. (2023). curs T.E.A.N. În capitolul 4.2.
[5]Obreja, D. (2023). curs T.E.A.N. În capitolul 9.
[6]Obreja, D. (2023). curs T.E.A.N. În capitolul 3.4.
[7]Obreja, D. (2023). curs T.E.A.N. În capitolul 3.4.

[8](***). Preluat de pe https://wind.willyweather.com/wa/jefferson-county/strait-of-juan-de-fuca.html

[9] Dan Obreja, (2021). Experimental techniques in the wind tunnel of Naval Architecture Faculty , The Annals of "Dunarea de Jos" University of Galati, Fascicle XI – Shipbuilding. ISSN 1221-4620, e-ISSN 2668-3156, 2021.

[10] Liviu Crudu, Radu Bosoancă, Radu Alexandru Mocanu, Dan Constantin Obreja, Costel Iulian Mocanu, Design and calibration of a six-component dynamometer used in an aerodynamic tunnel, The annals of "Dunarea de Jos" University of Galati, Fascicle XI – shipbuilding. ISSN 1221-4620, e-ISSN 2668-3156, DOI: https://doi.org/10.35219/AnnUgalShipBuilding/2022.45.01, 2022;

Paper received on November 10 th, 2025